To Be Decided

André Costa Batista, Ricardo Adriano, and Lucas S. Batista

***Abstract*—To be written.**

***Index Terms*—Keyword 1, keyword 2, keyword 3. Remember: alphabetical order.**

I. Introduction

HERE we go.

II. Problem Statement

Let $D \in \mathbb{R}^2$ denote the Domain of Interest (DOI) embedded within a homogeneous, isotropic, nonmagnetic ($\mu = \mu_0 = 4\pi \times 10^{-7}$ H/m), and lossless ($\sigma = \sigma_0 = 0$ S/m) background medium with permittivity $\epsilon_b = \epsilon_{rb}\epsilon_0$, where $\epsilon_0 \approx 8.85 \times 10^{-12}$ F/m. We consider a 2D Transverse Magnetic (TMz) polarization where the DOI is illuminated by incident plane waves and assume the time convention $e^{j\omega t}$. All scatterers are located within the DOI, and the scattered field E_z^s at point $\boldsymbol{\rho} \in S$ outside D is evaluated according to the following integral equation [1]:

$$E_z^s(\boldsymbol{\rho}) = -\frac{k_b^2}{4}\int_D H_0^{(2)}(k_b|\boldsymbol{\rho}-\boldsymbol{\rho'}|)\chi(\boldsymbol{\rho'})E_z(\boldsymbol{\rho'})dS' \quad (1)$$

where $k_b = \omega\sqrt{\epsilon_b\mu_0} = 2\pi/\lambda_b$ is the background wave number, λ_b is the wavelength of the incident wave, $H_0^{(2)}$ is the zero-order Hankel function of the second kind, E_z is the total electric field in the DOI, and χ is the contrast function given by

$$\chi(\boldsymbol{\rho}) = \frac{\epsilon_r(\boldsymbol{\rho})}{\epsilon_{rb}} - 1 - j\frac{\sigma(\boldsymbol{\rho})}{\omega\epsilon_b}, \quad (2)$$

which maps the relative permittivity $\epsilon_r(\boldsymbol{\rho})$ and conductivity $\sigma(\boldsymbol{\rho})$ distributions within D. It should be noted that the term $(-jk_b^2/4)H_0^{(2)}(k_b|\boldsymbol{\rho}-\boldsymbol{\rho'}|)$ corresponds to the Green's function in free space.

In electromagnetic inverse scattering problems, we aim to recover the contrast function χ using a set of N_M measurements of the scattered field collected for each of the N_S sources. Additionally, E_z is also unknown in D and must be solved. For our formulation, the N_S sources correspond to N_S incidence angles of the plane wave, and the N_M measurements are taken at N_M points in S, arranged in a circular, equidistant array situated far from the center of the DOI by a radius R_O. By discretizing the DOI into $N_X \times N_Y = N$ pixels, the inverse problem is solved numerically according to the following equation:

$$E_{ms}^s = -\sum_{n=1}^{N} G_{mn}^S \chi_n E_{ns} \quad (3)$$

where G^S is given according to the Richmond discretization [2], [3]. Equation (3) can also be expressed in matrix form:

$$\mathbf{E^S} = \mathbf{G^S}\boldsymbol{\chi}\mathbf{E} \quad (4)$$

where $\mathbf{E^S}$ is the $N_M \times N_S$ scattered field matrix, $\mathbf{G^S}$ is the $N_M \times N$ Green's function matrix, $\boldsymbol{\chi}$ is the $N \times N$ contrast diagonal matrix, and $\mathbf{E}$ is the $N \times N_S$ total electric field matrix.

It is important to highlight that, although assumptions are made regarding the scattered field domain and the incident field, the proposed indicators do not depend on these assumptions. They can be applied in any scenario where these entities are defined, and the assumptions in this paper serve only to clearly establish the context in which the indicators are tested.

III. Indicators

Once the result of the contrast function reconstruction is obtained by a given algorithm, the error in recovering the shape and location of the objects can be measured by comparing it with the original images. This means that the application of these metrics is relevant in studies where the exact response is known. Although in many real-world scenarios the imaged scatterer is unknown, applying these metrics to known cases can be valuable for comparing the performance of different algorithms and for estimating a confidence interval for the average performance of an algorithm in a given configuration. Therefore, these metrics are relevant tools that can contribute to the investigation and evaluation of algorithms for the problem.

For the two indicators that will be explained below, the image of the original contrast function of the problem and the image reconstructed by any algorithm will be denoted by the matrices $\bar{\boldsymbol{\chi}}_{\boldsymbol{o}}$ and $\bar{\boldsymbol{\chi}}_{\boldsymbol{r}}$, both of size $N_X \times N_Y$. In other words, the elements of these matrices represent the pixels of the images.

A. Shape Error

The contrast function has complex values when the medium or the scatterers have losses. Therefore, the first step is to account for the possibility that the elements of the matrices $\bar{\boldsymbol{\chi}}_{\boldsymbol{o}}$ and $\bar{\boldsymbol{\chi}}_{\boldsymbol{r}}$ have real and imaginary parts. The simplest approach is to use the magnitude of the complex variables as the value of each pixel. This choice does not eliminate the possibility that objects with different contrasts might have

This work has been supported by the Brazilian agencies Coordination for the Improvement of Higher Education Personnel - Brazil (CAPES) through the Academic Excellence Program (PROEX) under Grant 88887.815891/2023-00, FAPEMIG (Research Support Foundation of the State of Minas Gerais), and CNPq (The National Council for Scientific and Technological Development).

A. C. Batista, R. Adriano, and L. S. Batista are with the Department of Electrical Engineering, Universidade Federal de Minas Gerais, Belo Horizonte, MG 31270-901, Brazil (e-mail: andre-costa@ufmg.br; rluiz@ufmg.br; lusoba@ufmg.br). A. C. Batista and L. S. Batista are also with Operations Research and Complex Systems Laboratory (ORCS Lab), Belo Horizonte, MG, Brazil.

the same magnitude. However, in cases involving only lossless materials, this approach is not problematic because the contrast is purely real. Since the primary objective is to verify the shape of the scatterers, the critical aspect is distinguishing between the background medium and the scatterer, with the background medium having zero contrast. Thus, this approach to simplifying the methodology for measuring shape error should not have significant consequences in performance verification scenarios for the algorithm.

The contrast function reconstructed by many algorithms – such as BIM, DBIM, CSI, SOM, among others – is commonly a discretized approximation of a continuous surface. Therefore, even if the original image contains only objects with well-defined boundaries and homogeneous contrast, the image of these objects obtained by the algorithms will have frequently smooth edges, i.e., the contrast value gradually varies between the background medium and the object's value. Consequently, identifying a contour in the resulting image is heuristic because it requires selecting a criterion to define the contrast value at which a pixel can be considered as belonging to the object. For simplicity, the threshold T for considering a pixel in the recovered image to be within an object's contour will be defined as half of the total contrast variation in the image, i.e.:

$$T = \min(|\bar{\boldsymbol{\chi}}_{\boldsymbol{r}}|) + \frac{1}{2}\left[\max(|\bar{\boldsymbol{\chi}}_{\boldsymbol{r}}|) - \min(|\bar{\boldsymbol{\chi}}_{\boldsymbol{r}}|)\right] \tag{5}$$

This approach has advantages and disadvantages. If the reconstructed image contains multiple scatterers, and one or more of them has a contrast below this threshold, the methodology will fail to detect the contour of these objects. However, in scenarios where there is only one scatterer in the image, this approach is simple and effective. In fact, a single scatterer is the most objective way to test an algorithm's potential in recovering geometry, since the presence of multiple scatterers can degrade the algorithm's performance due to the influence of the induced currents in each scatterer on the scattering of the other. Furthermore, this approach poses no issues for algorithms capable of accurately capturing contours, such as machine learning-based methods. Moreover, instead of using the values from the original image, it is more beneficial to use only the values from the reconstructed image, both to isolate the influence of error in the contrast estimate and to apply the metric to qualitative methods that do not estimate contrast. If, for some reason, the original contrast function involves soft boundaries of the objects, the threshold might also be applied to the original image.

Once the thresholding step is applied, the contours of the scatterers can be determined. One of the techniques suitable for this task is the Marching Squares algorithm [4]. This algorithm efficiently returns a set of points that delineate each contour. It is important to note that hollow objects may have two or more contours. Additionally, if the imaging algorithm fails to detect an object, a discrepancy will arise in the number of contours between the original and reconstructed images.

For these reasons, instead of comparing the geometries through calculations based on the points of each contour, we prefer to perform the comparison based on the number of pixels that were misclassified. Specifically, after identifying which pixels fall within each contour in each image, we can determine which pixels belonged to the scatterers in the original image but were not captured in the reconstructed image (false negatives) and which pixels did not belong to the scatterers in the original image but were classified as such in the reconstructed image (false positives).

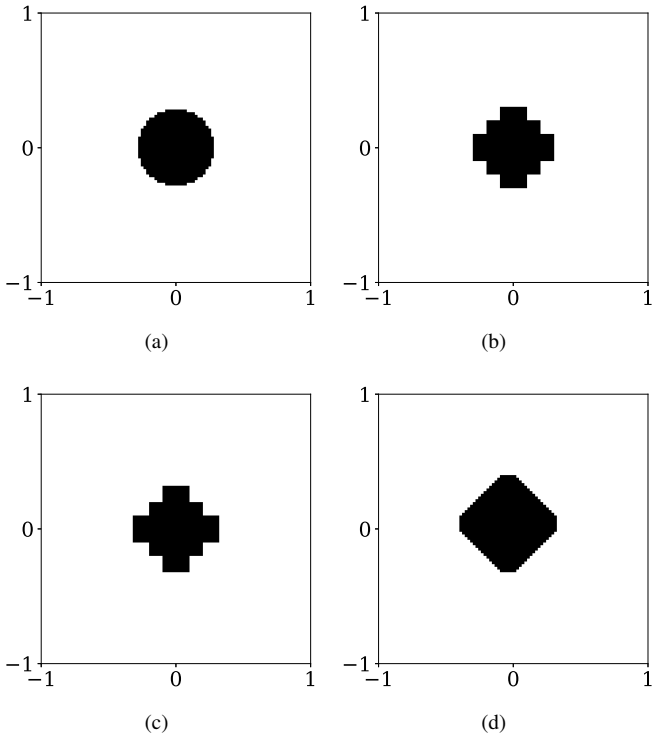

Fig. 1. An example illustrating the differences between nearest neighbor interpolation and the adopted contour detection methodology. (a) Original image of the scatterer (resolution 100x100); (b) Image reconstructed by an imaging algorithm after thresholding (20x20); (c) Image reconstructed to the original resolution using nearest neighbor interpolation; (d) Image reconstructed to the original resolution using contour identification.

A potential question that may arise from this choice is why not directly calculate false positives and false negatives immediately after thresholding. One reason is that original and reconstructed images typically have different resolutions. While the nearest neighbor interpolation method is an alternative for addressing this issue, the chosen approach may be more effective for capturing and preserving object contours, particularly when the resolution of the reconstructed image is significantly lower. This is illustrated in Fig. 1.

The sum of false negatives and false positives can be easily obtained by applying the XOR operation between the two images. Then, we can compute the shape error as the ratio between the number of incorrectly classified pixels and the total number of pixels that are part of the scatterers in the original image. Additionally, if we consider the shape error in percentage values, we can then define the indicator ζ_S as

$$\zeta_S = \frac{\text{FP} + \text{FN}}{\text{TP}} \times 100\%, \tag{6}$$

where FP and FN are the numbers of false-positive and false-negative pixels, respectively, and TP is the total number of

pixels that are part of the scatterers in the original image. Therefore, the indicator assumes values greater than or equal to zero. Note that values greater than 100% are also possible, indicating that the reconstructed image has more incorrectly classified pixels than the total number of pixels that make up the scatterers in the original image. This can occur more frequently when the number of pixels of the scatterer in the original image is small.

B. Position Error

The methodology for calculating the position detection error shares similarities with that of shape error calculation. As it is done when computing the shape error, the position error calculation also uses the absolute value of the image contrasts and applies the same thresholding operation. The reasons for this approach are the same.

The key difference lies in the method of position error calculation, which is based on comparing the centroid of pixels classified as objects by the thresholding operation in each image. Specifically, the centroid for each image is determined by averaging the coordinates of the pixels that constitute the objects. This method does not require contour detection, as the coordinate points are within the same boundaries for both images, even when resolutions differ.

The position error indicator is then defined as the Euclidean distance between the centroids in the two images. It is important to note that these centroids are normalized within a range of 0 to 1, where 0 represents the image's origin and 1 represents its end. By multiplying this distance by 100, the error can be interpreted as a percentage relative to the image size. Thus, the indicator quantifies the error in object localization relative to the image size, allowing its application across test sets with varying domain sizes. Therefore, the position error indicator ζ_P is defined as:

$$\zeta_P = \sqrt{(x_c^R - x_c^O)^2 + (y_c^R - y_c^O)^2} \times 100\%, \qquad (7)$$

where (x_c^R, y_c^R) and (x_c^O, y_c^O) are the centroids of the reconstructed and original images, respectively.

It should be noted that inaccuracies in the reconstructed geometry of objects can significantly influence the position error calculation. For example, if a star-shaped object with five points is reconstructed with one point distorted, this distortion will affect the object's centroid, thereby impacting the position error. However, this effect is expected, as any criterion for determining an object's position inherently considers the pixels defining it, as it is for its geometry. Furthermore, the proposed indicator is straightforward and versatile, applicable even in scenarios involving images with multiple objects.

IV. Computational Experiments

The experiments presented in this article are intended to illustrate the application of the proposed indicators. The design of these experiments focuses on demonstrating the potential utility of these indicators, rather than achieving pioneering results in the field. Nevertheless, the findings from these experiments can still provide a foundation for further research by the scientific community.

The experiments were conducted using the open-source library EISPY2D [5], specifically developed to design and evaluate algorithms for the inverse electromagnetic scattering problem. Both indicators will be analyzed, with each approach featuring two case studies (one fundamental and the other exploring a particular aspect) as well as a benchmarking study. The case studies aim to assess performance in specific scenarios, while the benchmarking study facilitates broader generalization of the results.

Para todos os experimentos, o λ_b foi definido em 1 [m]. O ruído acrescentado nos dados sempre foi de 5%. A permissividade relativa do meio de fundo sempre foi fixada em 1. A amplitude da onda incidente sempre foi fixada em 1 [V/m].

A. Shape Recovering Study

Para estudar o erro de forma, dois estudos de caso foram realizados. O primeiro estudo de caso consiste em um único espalhador com contraste homogêneo. O segundo estudo de caso envolve um espalhador com contraste variável. Ambos estudos de caso foram escolhidos para ilustrar a aplicação do indicador proposto em cenários comuns em problemas de espalhamento eletromagnético. O estudo de benchmarking foi realizado para medir o desempenho médio dos algoritmos em situações mais gerais.

Em todos os casos, as dimensões do DoI foram ajustadas para $2\lambda_b \times 2\lambda_b$. O raio de distância dos pontos de medição R_O foi fixado em $4\lambda_b$.

1) Single scatter: O primeiro estudo de caso foi formulado com objetivo de verificar a aplicabilidade do indicador em um cenário simples, onde diferentes algoritmos pudessem ser aplicados. O estudo considera um espelhador com formato de uma estrela de cinco pontas posicionada no centro da imagem. Esta escolha foi feita com o objetivo de escolher uma geometria que, ao mesmo tempo que é simétrica e bem definida, possui um número maior de vértices que geometria mais comuns, como quadrados ou triângulos. O contraste foi fixado em 0.25 e o raio do centro do espalhador até os vértices mais distantes foi fixado em $0.9\lambda_b$. Foram considerados 80 pontos de medição (N_M) e 80 ângulos de incidência (N_S).

2) Varying contrast:

3) Average performance:

B. Position Detection Study

1) Single scatter:

2) Multiple scatterers:

3) Average performance:

V. Conclusion

A conclusion section is not required. Although a conclusion may review the main points of the paper, do not replicate the abstract as the conclusion. A conclusion might elaborate on the importance of the work or suggest applications and extensions. [6]

ACKNOWLEDGMENT

Use the singular heading even if you have many acknowledgments. In most cases, sponsor and financial support acknowledgments are placed in the unnumbered footnote on the first page, not here.

REFERENCES

[1] R. F. Harrington, *Time-Harmonic Electromagnetic Fields*. Wiley-IEEE Press, 2001.

[2] J. Richmond, "Scattering by a dielectric cylinder of arbitrary cross section shape," *IEEE Transactions on Antennas and Propagation*, vol. 13, no. 3, pp. 334–341, 1965.

[3] *The Electromagnetic Inverse Scattering Problem*. John Wiley & Sons, Ltd, 2010, ch. Three, pp. 20–56. [Online]. Available: https://onlinelibrary.wiley.com/doi/abs/10.1002/9780470602492.ch3

[4] W. E. Lorensen and H. E. Cline, "Marching cubes: A high resolution 3d surface construction algorithm," in *Proceedings of the 14th Annual Conference on Computer Graphics and Interactive Techniques*, ser. SIGGRAPH '87. New York, NY, USA: Association for Computing Machinery, 1987, p. 163–169. [Online]. Available: https://doi.org/10.1145/37401.37422

[5] A. C. Batista, R. Adriano, and L. S. Batista, "Eispy2d: An open-source python library for the development and comparison of algorithms in two-dimensional electromagnetic inverse scattering problems," 2022. [Online]. Available: https://arxiv.org/abs/2111.02185

[6] X. Chen, *Computational methods for electromagnetic inverse scattering*. Wiley Online Library, 2018, vol. 244.